Epitaxial growth of ultra-thin NbN films on $Al_xGa_{1-x}N$ buffer-layers

2014 Supercond. Sci. Technol. 27 065009

(http://iopscience.iop.org/0953-2048/27/6/065009)

IOP Publishing Superconductor Science and Technology
Supercond. Sci. Technol. **27** (2014) 065009 (7pp) doi:10.1088/0953-2048/27/6/065009

Epitaxial growth of ultra-thin NbN films on $Al_xGa_{1-x}N$ buffer-layers

S Krause[1], D Meledin[1], V Desmaris[1], A Pavolotsky[1], V Belitsky[1], M Rudziński[2] and E Pippel[3]

[1] Group for Advanced Receiver Development, Chalmers University of Technology, SE-412 96 Gothenburg, Sweden
[2] Institute of Electronic Materials Technology (ITME), 01-919 Warsaw, Poland
[3] Max Planck Institute of Microstructure Physics, D-06120 Halle/Saale, Germany

E-mail: sascha.krause@chalmers.se

Received 11 November 2013, revised 4 February 2014
Accepted for publication 3 March 2014
Published 8 April 2014

Abstract

The suitability of $Al_xGa_{1-x}N$ epilayers to deposit onto ultra-thin NbN films has been demonstrated for the first time. High quality single-crystal films with 5 nm thickness confirmed by high resolution transmission electron microscopy (HRTEM) have been deposited in a reproducible manner by means of reactive DC magnetron sputtering at elevated temperatures and exhibit critical temperatures (T_c) as high as 13.2 K and residual resistivity ratio (RRR) ~1 on hexagonal GaN epilayers. On increasing the Al content x in the $Al_xGa_{1-x}N$ epilayer above 20%, a gradual deterioration of T_c to 10 K was observed. Deposition of NbN on bare silicon substrates served as a reference and comparison. Excellent spatial homogeneity of the fabricated films was confirmed by $R(T)$ measurements of patterned micro-bridges across the entire film area. The superconducting properties of these films were further characterized by critical magnetic field and critical current measurements. It is expected that the employment of GaN material as a buffer-layer for the deposition of ultra-thin NbN films will prospectively benefit terahertz electronics, particularly hot electron bolometer (HEB) mixers.

Keywords: NbN, ultra-thin films, HEB

(Some figures may appear in colour only in the online journal)

1. Introduction

Hot electron bolometer (HEB) based heterodyne receivers have been shown to be the most sensitive detectors for spectroscopy in the terahertz frequency range above 1.3 THz [1–3], and are essential for radio astronomical instrumentation [4]. Such phonon-cooled HEB-based mixers widely employ NbN as superconducting material for the bolometers, exploiting short electron–phonon and phonon-escape interaction times that yield a decent intermediate frequency (IF) band. The performance of such devices is intrinsically associated with the superconducting properties of the film, such as the critical temperature (T_c) at which the phase transition from the resistive to the superconducting state occurs, as well as the film thickness [5, 6], whereby higher T_c and thinner films are desirable. The challenge of achieving ultimate IF bandwidth is posed by the reduction of T_c from 16 to 17 K of the bulk material and increase in sheet resistance (R_{sheet}) when approaching film thicknesses in the range of a few nanometers [7]. Besides careful optimization of NbN deposition process parameters, the choice of substrate on which to grow NbN is crucial for achieving the high T_c and thus high quality 3.5–6 nm thin films required for HEBs.

The use of a silicon substrate is commonly adopted and features advantageous properties from a processing point of view as well as relatively low losses at THz frequencies. However, due to the significant lattice mismatch to NbN, only polycrystalline films, not exceeding a T_c of approximately 10 K at 5 nm thickness, have been demonstrated [2, 8, 9]. In order to increase the T_c, and hence the superconducting quality of the NbN ultra-thin films, substrates with low lattice mismatch to NbN such as MgO [10–12], sapphire [13]

and the recently demonstrated 3C-SiC have been utilized and provide an epitaxial growth resulting in increased T_c, e.g. 11.8 K [14, 15]. Processing and life-time issues arise with the use of MgO as a buffer-layer due to its hydrophobic nature and sensitivity to alkaline solutions. Bulk sapphire substrates on the other hand introduce challenges due to their hardness and restrict particularly THz waveguide applications.

Therefore the use of alternative buffer-layers, which could be grown on silicon and still provide a close lattice match to NbN, is the most attractive solution from the perspective of device fabrication and system integration. The crystallographic orientation of the NbN film does not influence its superconducting properties. As a result, the c-plane of hexagonal buffer-layers would also be suitable providing that their lattice parameter a matched that of NbN oriented along its (111) direction, i.e. $a_{111} = a_{100}/\sqrt{2}$, and thus yielded a crystallographic alignment to AlGaN in its (0001) direction. In this paper, we describe the growth of single-crystal ultra-thin NbN films onto hexagonal $Al_xGa_{1-x}N$ substrates by means of reactive DC magnetron sputtering. An extensive characterization of the processed films has been performed, including fabrication of micro-bridges, film homogeneity studies, and $R(T)$ to study the superconducting transition. Furthermore, the crystallographic quality of the films was characterized by high resolution transmission electron microscopy (HRTEM) and high angle annular dark field detector/scanning transmission electron microscopy (HAADF/STEM). The results for the NbN/AlGaN compound strongly point towards prospective applications in THz electronics, particularly HEB mixers and circuitry that takes advantage of the enhanced superconducting properties of epitaxially grown NbN films.

2. Experiment

The 1.2 and 2 μm thick $Al_xGa_{1-x}N$ wurtzite epilayers were grown onto 2 in c-plane sapphire (0001) substrates by metal–organic chemical vapor deposition (MOCVD) using an RF heated AIX200/4RF-S low pressure horizontal reactor. High quality AlGaN layers with low defect densities are typically obtained above 1 μm thickness; however, they can be grown much thicker. The use of sapphire as a substrate on which to grow AlGaN for initial experiments is motivated by its wide availability. In order to validate that the sapphire substrate exerts no influence on the growth of the NbN ultra-thin film on the AlGaN epilayer, NbN was also deposited onto the GaN buffer-layer, which was itself grown onto bare silicon substrates with no considerable disorientation.

Samples with different Al contents x ranging from 0% (GaN) to 100% (AlN) were prepared, and yielded a shift in the lattice constant from $a_{\text{w-GaN}} = 3.189$ Å to $a_{\text{w-AlN}} = 3.11$ Å. It is expected that by changing the Al content the lattice constant of the cubic δ-NbN phase in its (111)-orientation can be perfectly matched. In addition, AlGaN features a dielectric constant ε_r lower than that of Si, ranging from 8.5 to 9.5 for AlN and GaN respectively [16], making them applicable in membrane-like structures, i.e. waveguide-based THz applications. The power absorption of epitaxial GaN in the frequency range of 0.1–4 THz was reported in [17] and

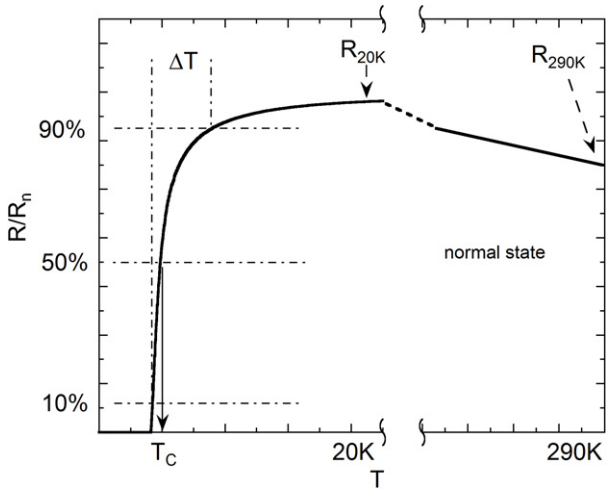

Figure 1. Typical resistance versus temperature behavior of ultra-thin NbN films and indicated figure of merit for assessing the quality of the films.

shows a similar behavior to that of p-type silicon (0.92 Ω cm) at room temperature [18]. Considering that the intended THz application operates at cryogenic temperatures, the losses introduced by the epilayer and substrate will be even smaller, if not negligible.

The deposition of NbN ultra-thin films was performed by means of reactive DC magnetron sputtering using an AJA Orion-6UD sputtering tool. The system contains a high-purity 2 in Nb target and is able to achieve a base pressure of 1.8×10^{-8} Torr in the process chamber. Prior to loading, all substrates were ultrasonically cleaned in acetone, rinsed with isopropanol and subsequently dry-blown in nitrogen. No further treatment of the surface of bare silicon samples was applied, implying that the native oxide layer remained. The substrate holder was pre-heated to either 525 or 650 °C and maintained at this temperature during the sputtering. Furthermore, applied pre-conditioning of the target by excessive sputtering with a closed shutter provided a reliable deposition process. The partial pressure of argon and nitrogen was carefully adjusted and best results were achieved when keeping the ratio N_2/Ar close to 1:9.2 at a fixed DC magnetron current of 0.5 A at 2.8 mTorr ambient pressure. The deposition rate resulting for these conditions is approximately 1.2 Å s^{-1} and was deduced from HRTEM and ellipsometry characterizations. Moreover, additional depositions of NbN films on bare silicon wafers with studied superconducting properties were carried out and indicated eventual changes in the quality of the deposition process.

All deposited films were subjected to resistance–temperature $R(T)$ measurement in a temperature-calibrated four-point-probe setup. The typical behavior of the resistance as a function of temperature of thin NbN films is illustrated in figure 1. The critical temperature T_c is associated with the transition to the superconducting state and corresponds to a drop of resistance to 50% of its normal-state value, whereas the transition width ΔT is taken from 90 to 10% of the normal-state resistance. A narrow transition width is evidence of high quality structural properties and benefits the sensitivity

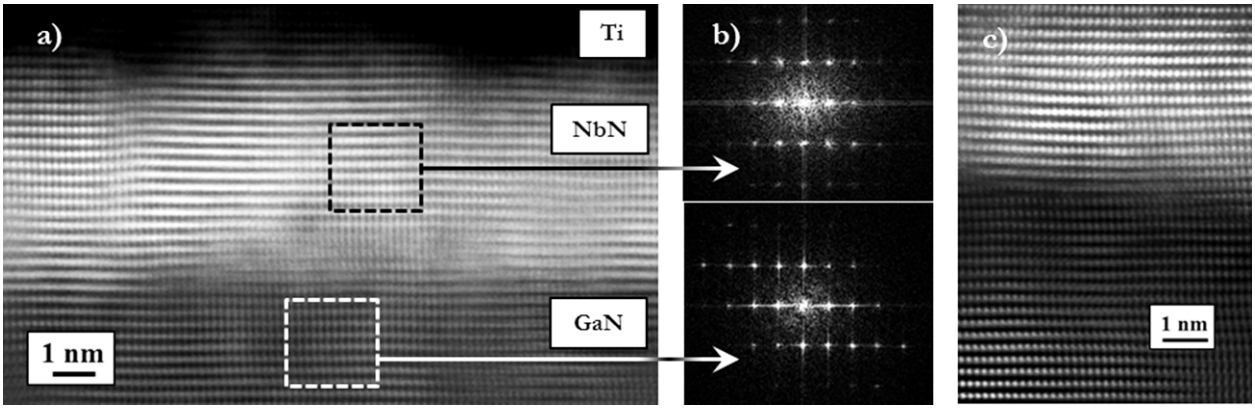

Figure 2. Single-crystal NbN on GaN epilayer in cross-sectional HAADF/STEM image. (a) Ti/NbN/GaN layer system confirming thickness of approximately 5 nm. (b) Diffraction pattern by FFT of selected areas. (c) NbN/GaN interface with no signs of diffusion.

of e.g. HEB devices. The residual resistivity ratio (RRR) is commonly defined as the ratio of film resistance at room temperature and at 20 K for NbN.

More related to prospective devices is the validation of aforementioned properties on a microscopic scale. Thus, micro-bridges with varying bridge dimensions from 5×5 to 4×20 μm^2 distributed over the entire film area were fabricated, probed and re-measured. From this measurement, the uniformity was deduced by locally assessing the deviation of T_c and R_{sheet}. The described micro-bridges were within the accuracy of photo-lithography techniques and defined by dry etching in CF_4, whereas electrical leads and contact pads consist of sputtered Nb, Al and Pd (20/250/150 nm) layers in order to provide good adhesion to NbN, low electrical resistance above T_c and an easy bond ability.

Furthermore, critical current and upper critical magnetic field measurements under applied magnetic field ranging from 0 to 15 T have been conducted and superconducting parameters such as zero-field critical current density J_{c0}, second critical magnetic field $\mu_0 H_{c2}$ and electron diffusion constant D were determined. HRTEM images taken by a TITAN 80-300 accurately verified the fabricated film thickness, whereas HAADF/STEM analysis was employed to assess the interface of NbN and epilayers as well as revealing crystallographic properties from diffraction patterns obtained by Fourier transformation. In the following, the presented HRTEM analysis was conducted on processed micro-bolometers after their comprehensive electrical characterization. The prepared specimens were taken from ultra-thin NbN films deposited on GaN and $Al_{0.54}Ga_{0.46}N$ buffer-layers, which were grown onto sapphire substrates, and NbN on bare silicon as comparison. Prior the preparation of the specimen, an additional Ti/Au (20/200 nm) layer was evaporated onto the NbN in order to provide a sufficient contrast and to protect the surface from eventual damage.

3. Results and discussion

3.1. NbN on GaN buffer-layer

As seen in figure 2(a), there is clear evidence of the epitaxial single-crystal growth of NbN on the GaN buffer in its (111)-orientation. The expected film thickness of 5 nm, adequate for application requirements, i.e. HEB mixers, has been confirmed according to the provided scale; the film thickness is reasonably constant across the entire cross-section. Furthermore, the diffraction patterns taken by fast Fourier transformation (FFT) from NbN and GaN structures coincide and support the very low lattice mismatch as illustrated in figure 2(b). The interface across NbN/GaN exhibits a sharp transition within one atomic layer with very few defects, thus indicating that no inter-diffusion has taken place while depositing at elevated substrate temperatures. Moreover, the high quality of the NbN/GaN interface may improve the phonon transmissivity [19] and thus particularly benefit the enhancement of phonon-cooled HEBs' IF bandwidth.

3.2. NbN on AlGaN buffer-layer

In order to study the influence of Al content in the employed $Al_xGa_{1-x}N$ buffer-layers on the quality of NbN films, another specimen with a NbN/$Al_{0.54}Ga_{0.46}N$ compound has been prepared and characterized by HRTEM, HAADF/STEM and FFT. As illustrated in figure 3(a), the NbN film grown onto the AlGaN layer exhibits a mono-crystalline structure with some stacking defects. The film thickness of approximately 5 nm is verified across the cross-section. The FFT as shown in figure 3(b) points to the fact that the lattice mismatch is slightly increased, since the diffraction patterns do not coincide perfectly. Furthermore, it is observed in figure 3(c) that the AlGaN/NbN interface is not as sharp as that for GaN and features a lower atomic mass, indicated in the Z-contrast HAADF/STEM image as a dark region. The origin of this disordered layer is uncertain. We presume that oxidation on the surface has taken place [20], which is more likely to happen with increasing Al content. However, the forming of lighter compounds of Al at elevated substrate temperatures or defects introduced by selective sputter-cleaning are also conceivable.

3.3. NbN on silicon substrate

In comparison to the above presented epitaxially grown films, the cross-section of NbN deposited on bare silicon wafer with

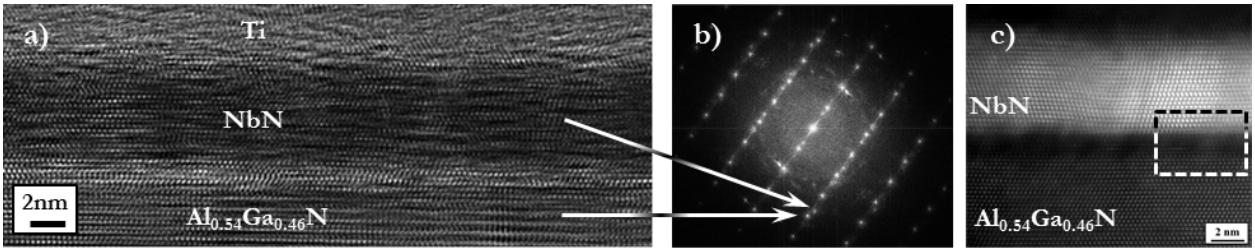

Figure 3. (a) Cross-section of epitaxially grown NbN film on $Al_{0.54}Ga_{0.46}N$ layer in HRTEM image. (b) Superimposed diffraction pattern by FFT taken from AlGaN and NbN. (c) HAADF/STEM reveals a lighter and disordered layer across the film/substrate interface, seen as the black region.

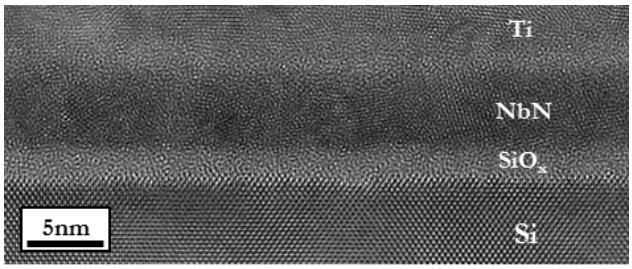

Figure 4. HRTEM image of NbN grown onto silicon with native amorphous SiO_x layer. The polycrystalline structure is clearly pronounced, in contrast to those on AlGaN due to the large lattice mismatch.

a native oxide layer of approximately 2 nm is depicted in figure 4. The polycrystalline structure and the arrangement in differently sized grains is clearly visible and in contrast to those on GaN and AlGaN samples.

3.4. Critical temperature and RRR

All samples were separately mounted on a four-point-probe fixture with closely attached temperature sensor and slowly dipped into the LHe (liquid helium) Dewar. A critical temperature as high as 13.2 K with narrow transition width has been attained for NbN films deposited onto the GaN buffer-layer at the substrate holder temperature of 650 °C. Figure 5 summarizes the results of current and previous reported studies on commonly employed buffer-layers for the growth of NbN ultra-thin films and indicates the increase in T_c by 10% compared to MgO layers. Furthermore, NbN was simultaneously deposited at 525 °C onto the GaN buffer-layer; which itself was grown both onto sapphire substrate and bare silicon. The critical temperatures reached for these films are similar and amount to 13 and 12.8 K, respectively. Thus, eventual effects of the underlying sapphire substrates on the growth of NbN can be excluded, and the suitability of the thin GaN epilayer on silicon substrates has been demonstrated.

The Al content x in the $Al_xGa_{1-x}N$ composition clearly exerts influence on NbN superconducting properties such as the gradual degradation of T_c involving a rise in R_{sheet} when increasing x above 20% as illustrated in figure 6(a). The sheet resistance was calculated upon known sample geometry and area size [23]. It is also worth noting that R_{sheet} of NbN on the GaN layer is almost half of that measured for NbN

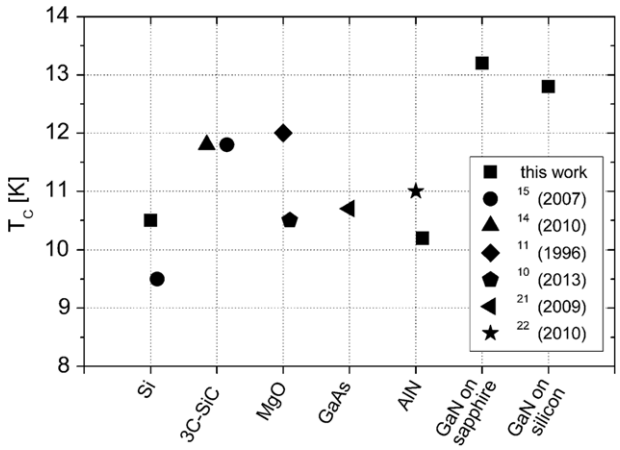

Figure 5. Current state-of-the-art NbN ultra-thin films with thicknesses ranging from 3.5 to 6 nm grown on different buffer-layers.

deposited onto the AlN epilayer and significantly lower than that deposited onto bare silicon.

The RRR is considered an important figure of merit for providing information on structural properties such as disorder, and is unity in the case of bulk NbN [24, 25]. Figure 6(b) depicts RRR as a function of increasing Al content in comparison with silicon substrate grown at two different temperatures. The RRR close to unity for GaN epilayers is evidence for an epitaxial growth as confirmed by HRTEM. Moreover, the RRR gradually decreases with increasing Al content and complements the deterioration of the films' T_c. The slight shift in the curves for 650 and 525 °C may be attributed to greater contamination with impurities, resulting in lower RRR due to the increased outgassing at higher substrate holder temperatures.

3.5. Film uniformity

At least 10 micro-bridges distributed across the entire wafer area were manufactured and characterized by $R(T)$ measurements in a dedicated laboratory arrangement. It should be mentioned that all films were stored in ambient atmosphere for up to one month before they were processed. Nevertheless, re-measuring of randomly chosen samples has shown that the superconducting properties such as T_c and R_{sheet} are scarcely degraded.

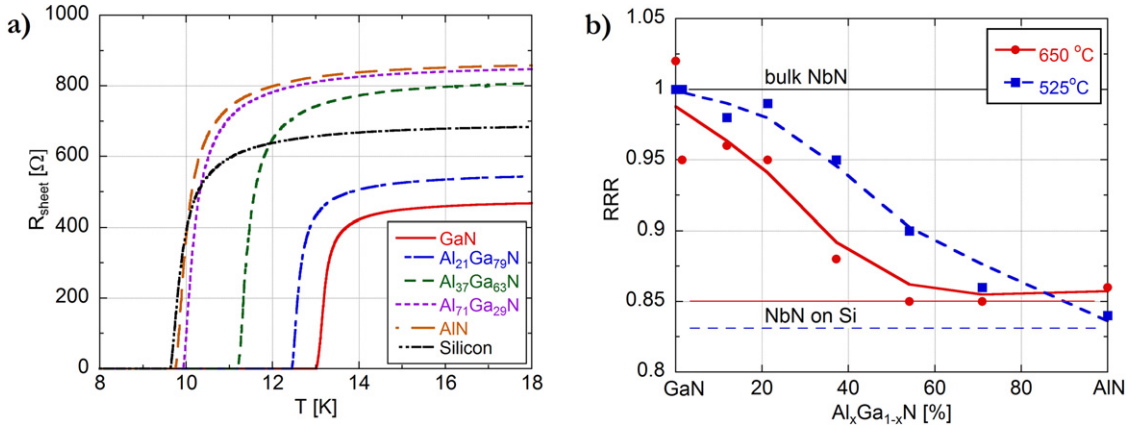

Figure 6. (a) Sheet resistance of NbN grown at 650 °C onto $Al_xGa_{1-x}N$/sapphire substrates as a function of temperature for different Al contents in comparison with bare silicon. (b) RRR versus Al content for deposition at 525 and 650 °C.

After processing, the measured T_c of the NbN films on the GaN buffer-layer remained as high as 12.83 K. The standard deviation of the sheet resistance, R_{sheet}, indicates homogeneous films and is markedly low, from 3.5 to 4.8% for epitaxially grown NbN films on AlGaN buffer-layers. In contrast, the corresponding standard deviations of the sheet resistance for polycrystalline films on silicon and $Al_{>0.54}Ga_{<0.46}N$ are twice as high. The deterioration of T_c from 12.83 to 10 K and broadening of the superconducting transition width ΔT_c with increasing Al content is distinct. Moreover, the data presented in table 1 confirm high film uniformity and give evidence that no damage has been introduced into the films due to the processing of micro-bridges.

3.6. Critical current and magnetic field measurement

Prior to preparing the samples for HRTEM, critical magnetic field and critical current measurements were carried out on NbN micro-bridges on GaN, $Al_{0.54}Ga_{0.46}N$ and silicon substrates with dimensions of 5 nm × 10 μm × 70 μm in thickness, width and length, respectively. Figure 7(a) depicts the dependence of critical current on temperature. The measured data were fitted by applying the simplified Ginzburg–Landau relationship [26], and shows satisfactory agreement. The extracted critical current density J_{c0} amounts to 3.8 MA cm^{-2} for NbN films deposited on GaN buffer-layers and deteriorates to 1.2 MA cm^{-2} for the films on bare silicon. These results agree well with other reported results on polycrystalline films of similar thicknesses [14]. The extracted critical current density for $Al_{0.54}Ga_{0.46}N$ of $J_{c0} =$ 2.1 MA cm^{-2} falls between the current density of the NbN films deposited onto the GaN buffer-layer and silicon. The critical magnetic field measurements as seen in figure 7(b) allow for the estimation of diffusion constants in the ultra-thin NbN film [27].

$$D = -\frac{0.407\pi k_B}{e}\left(\frac{d\mu_0 H_{c2}}{dT}\right)^{-1}. \quad (1)$$

Applying the derivative of the critical magnetic field over the temperature in the vicinity of zero-field T_{c0} according to (1) yielded a diffusion constant on silicon substrates of approximately 0.41 cm^2 s^{-1}, which agrees well with the value of 0.4 cm^2 s^{-1} reported [28]. In contrast, the diffusion constant extracted for NbN on a GaN buffer-layer is significantly enhanced and reaches 0.63 cm^2 s^{-1}, confirming the improved structural properties such as high order and low defect density. This can particularly be employed in utilizing an additional diffusion-cooling channel in phonon-cooled HEB mixers in order to further increase the IF bandwidth, as recently demonstrated [29, 30].

4. Conclusion

We have successfully demonstrated the possibility of growing single-crystal epitaxial NbN films on $Al_xGa_{1-x}N$ ($x < 20\%$) buffer-layers by means of reactive DC magnetron sputtering. As a result, state-of-the-art ultra-thin NbN films on GaN buffer-layers with thickness of approximately 5 nm and high homogeneity confirmed by HRTEM and HAADF/STEM have been deposited with T_c as high as 13.2 K and RRR close to unity. Upon the fabrication of micro-bridges across the entire film area, $R(T)$ measurements revealed high film uniformity with the standard deviation of 3.5%–4.8% of the sheet resistance for NbN films deposited onto AlGaN substrates, whereas that on silicon amounted to 8%. Furthermore, the critical current density for NbN films grown onto the GaN buffer-layer is more than three times higher than for silicon substrates and amounts to 3.8 MA cm^{-2}. It has been observed that the superconducting properties gradually deteriorate when increasing the Al content of the $Al_xGa_{1-x}N$ composition above 20%, and eventually approach those of films deposited onto bare silicon. The diffusion constants deduced from critical magnetic field measurements are 0.63 cm^2 s^{-1} for NbN on a GaN buffer-layer compared to 0.41 cm^2 s^{-1} for NbN on silicon.

It is expected that the employment of GaN material as a buffer-layer for the deposition of ultra-thin NbN films will prospectively benefit terahertz electronics, particularly hot electron bolometer (HEB) mixers.

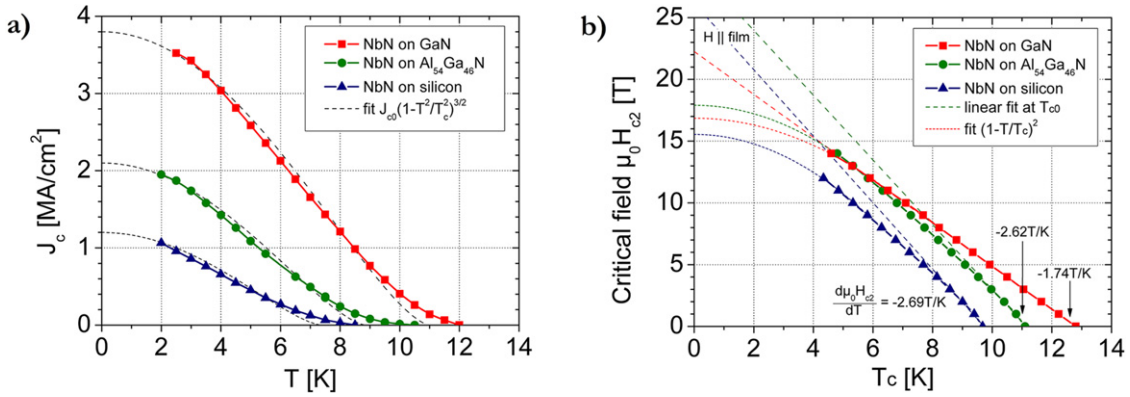

Figure 7. (a) Critical current density as a function of temperature for NbN on GaN and $Al_{0.54}Ga_{0.46}N$ substrate in comparison with silicon. The films were deposited at 625 °C and micro-bridges with dimensions of 5 nm × 10 μm × 70 μm fabricated. (b) Upper critical magnetic field versus T_c of GaN, $Al_{0.54}Ga_{0.46}N$ and silicon substrate with corresponding curve-fitting.

Table 1. Statistical summary, taken over ten samples measured on 5 nm thin NbN micro-bridges across the entire film area.

	Film as deposited		Patterned micro-bolometers		R_{sheet} at 20 K	
Buffer-layer/substrate	T_c (K)	ΔT_c (K)	T_c (K)	ΔT_c (K)	(Ω)	std (R_{sheet}) (%)
GaN	13.2	1.1	12.83 ± 0.04	1.38 ± 0.04	492 ± 20	4
$Al_{0.21}Ga_{0.79}N$	12.8	1.22	12.55 ± 0.07	1.54 ± 0.04	647 ± 23	3.5
$Al_{0.37}Ga_{0.63}N$	12.5	1.28	12.31 ± 0.02	1.57 ± 0.05	587 ± 26	4.8
$Al_{0.54}Ga_{0.46}N$	11.5	1.55	11.3 ± 0.05	1.86 ± 0.05	807 ± 35	4.3
$Al_{0.71}Ga_{0.29}N$	10.2	1.73	10.0 ± 0.12	2.02 ± 0.07	900 ± 81	9
Silicon	10.1	1.61	9.78 ± 0.02	1.91 ± 0.02	970 ± 85	8.8

Acknowledgments

The authors acknowledge Alexei Kalaboukhov at the Quantum Device Physics Laboratory, Chalmers University of Technology, for his conducted measurements of the critical current and second critical magnetic field of the ultra-thin NbN films. The work on the employed substrates with AlGaN buffer-layer was partially supported by the NCBR in the frame of project INNOTECH-K2/IN2/85/182066/NCBR/13, and by MRR in the frame of project POIG.01.01.02-00-015/09-00.

References

[1] Gershenzon E, Gol'tsman G, Gogidze I, Gusev Y, Eliantev A, Karasik B and Semenov A 1990 *Sov. Phys.—Supercond.* **3** 1582 (Engl. transl.)
Gershenzon E, Gol'tsman G, Gogidze I, Gusev Y, Eliantev A, Karasik B and Semenov A 1990 *Sverkhprovodimost: Fiz. Khim. Tekh.* **3** 2143
[2] Semenov A, Hübers H-W, Schubert J, Gol'tsman G, Elantiev A, Voronov B and Gershenzon E 2000 *J. Appl. Phys.* **88** 6758
[3] Meledin D *et al* 2009 *IEEE Trans. Microw. Theory Tech.* **57** 89
[4] Kulesa C 2011 Terahertz spectroscopy for astronomy: from comets to cosmology *IEEE Trans. THz Sci. Technol.* **1** 1
[5] Sergeev A and Reizer M 1996 Photoresponse mechanism of thin superconducting films and superconducting detectors *Int. J. Mod. Phys.* B **10** 635–67
[6] Il'in K, Lindgren M, Currie M, Semenov A, Gol'tsman G, Sobolewski R, Cherednichenko S and Gershenzon E 2000 Picosecond hot-electron energy relaxation in NbN superconducting photodetectors *Appl. Phys. Lett.* **76** 19
[7] Kang L, Jin B, Liu X, Jia X and Chen J 2011 Suppression of superconductivity in epitaxial NbN ultrathin films *J. Appl. Phys.* **109** 033908
[8] Cherednichenko S, Khosropanah P, Kollberg E, Kroug M and Merkel H 2002 *Physica* C **372** 427–31
[9] Gao J *et al* 2005 *Appl. Phys. Lett.* **86** 244104
[10] Kawakami A, Tanaka S, Yasui M, Hosako I and Irimajiri Y 2013 Design and fabrication of NbN terahertz hot electron bolometer mixers *24th Int. Symp. on Space Terahertz Technology*
[11] Wang Z, Kawakami A, Uzawa Y and Komiyama B 1996 Superconducting properties and crystal structures of singlecrystal niobium nitride thin films deposited at ambient substrate temperature *J. Appl. Phys.* **79** 7837
[12] Gol'tsman G *et al* 2005 *Proc. SPIE* **5727** 95–106
[13] Lamaestre R, Odier P, Bellet-Amalric E, Cavalier P, Pouget S and Villégier J-C 2008 High quality ultrathin NbN layers on sapphire for superconducting single photon detectors *J. Phys.: Conf. Ser.* **97** 012046
[14] Dochev D, Desmaris V, Pavolotsky A, Meledin D, Lai Z, Henry A, Janzén E, Pippel E, Woltersdorf J and Belitsky V 2011 Growth and characterization of epitaxial ultra-thin NbN films on 3C-SiC/Si substrates for terahertz applications *Supercond. Sci. Technol.* **24** 035016
[15] Gao J, Hajenius M, Tichelaar F, Klapwijk T, Voronov B, Grishin E, Gol'tsman G, Zorman C and Mehregany M 2007 Monocrystalline NbN nanofilms on a 3C-SiC/Si substrate *Appl. Phys. Lett.* **91** 062504

[16] Bougrov V, Levinshtein M, Rumyantsev S and Zubrilov A 2001 *Properties of Advanced Semiconductor Materials GaN, AlN, InN, BN, SiC, SiGe* (New York: Wiley) pp 1–30
[17] Zhang W, Azad A K and Grischkowsky D 2003 Terahertz studies of carrier dynamics and dielectric response of n-type, freestanding epitaxial GaN *Appl. Phys. Lett.* **82** 2841–3
[18] Träger F 2012 *Handbook of Lasers and Optics* 2nd edn (Berlin: Springer) p 1441
[19] Li X and Yang R 2012 Effect of lattice mismatch on phonon transmission and interface thermal conductance across dissimilar material interfaces *Phys. Rev.* B **86** 054305
[20] Edgar J, Du L, Lee R, Nyakiti L and Chaudhuri J 2008 Native oxide and hydroxides and their implication for bulk AlN crystal growth *J. Cryst. Growth* **310** 4002
[21] Marseli F, Gaggero A, Li L, Surrente A, Leoni R, Levy F and Fiore A 2009 High quality superconducting NbN thin films on GaAs *Supercond. Sci. Technol.* **22** 095013
[22] Shiino T, Shiba S, Sakai N, Yamakura T, Jiang L, Uzawa Y, Maezawa H and Yamamoto S 2010 *Supercond. Sci. Technol.* **23** 045004
[23] Smits F 1958 Measurement of sheet resistivities with the four-point probe *Bell Syst. Tech. J.* **37** 711
[24] Jones H 1975 *Appl. Phys. Lett.* **27** 471
[25] Marsili F, Bitauld D, Fiore A, Gaggero A, Mattioli F, Leoni R, Benkahoul M and Levy F 2008 *Opt. Express* **16** 3191
[26] Cyrot M 1973 Ginzburg–Landau theory for superconductors *Rep. Prog. Phys.* **36** 103
[27] Martins B 2006 *New Frontiers in Superconductivity Research* (New York: Nova Science) p 171
[28] Floet D, Gao J, Klapwijk T and Korte P 2001 Thermal time constant of Nb diffusion-cooled superconducting hot-electron bolometer mixers *IEEE Trans. Appl. Supercond.* **11** 187–90
[29] Ryabchun S, Tretyakov I, Finkel M, Maslennikov S, Kaurova N, Seleznev V, Voronov B and Gol'tsman G 2008 Fabrication and characterization of NbN HEB mixers with *in situ* gold contacts *19th Int. Symp. on Space Terahertz Technology*
[30] Finkel M, Vachtomin Y, Antipov S, Drakinski V, Kaurova N, Voronov B and Gol'tsman G 2003 Gain bandwidth and noise temperature of NbTiN HEB mixers *14th Int. Symp. on Space Terahertz Technology*